

SUPPLEMENTAL INFORMATION

SUPPLEMENTAL FIGURES

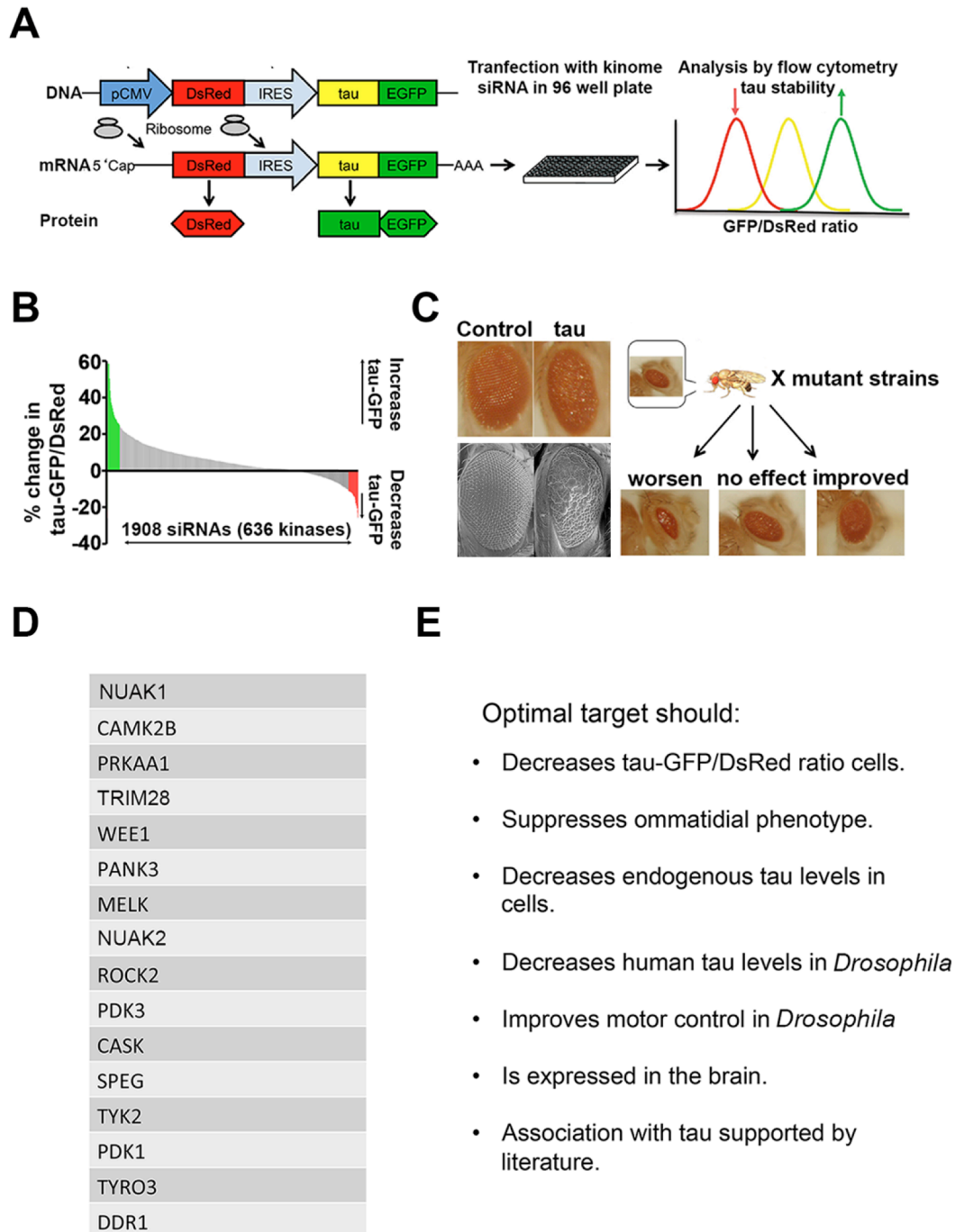


Figure S1, related to Fig. 1.: Cross-species genetic screening strategy to identify regulators of tau stability. **A)** Forward genetic screen strategy for modifiers of tau levels. DsRed-IRES-Tau-GFP expressing cells used to assess the abundance of tau by monitoring the Tau-GFP to DsRed fluorescence ratio. siRNAs that reduced tau protein lead to a decrease in Tau-GFP but not DsRed. **B)** Primary screen results showed the effect on average Tau-GFP/DsRed ratio per kinase siRNAs tested. **C)** Schematic of *Drosophila* screen for suppressors of tau-induced eye degeneration. **D)** List of 16 common modifiers obtained from the cell based and *Drosophila* screening. **E)** Criteria for pursuing further validation.

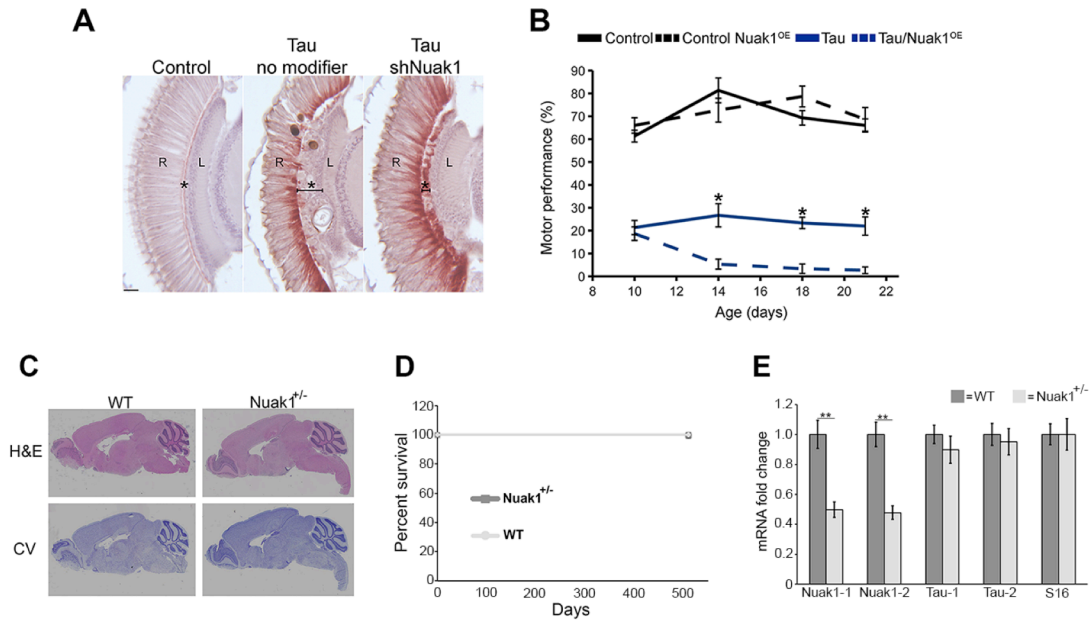


Figure S2, related to figure 1: Effects of Nuak1 *in vivo*. **A)** Paraffin cross-section images of *Drosophila* eyes from the indicated genotypes. Control flies show a very thin layer between the retina (R) and the lamina (L) regions, called the subretinal pigment layer (SPL, star). This layer contains axonal projections from the retina and cell bodies from lamina neurons and glial cells (Control). Expression of human tau in the retina leads to a significant swelling of the SPL (star), highlighted by the marker line (tau no modifier). Knocking down Nuak1 levels in the retina leads to a noticeable suppression of this tau-induced swelling (star and marker line in tau shNuak1). **B)** Nuak1 over-expression impairs motor performance as tau-expressing *Drosophila* age. Error bars, s.d.m. * $p < 0.05$. **C)** No gross abnormalities were observed in *Nuak1*^{+/-} brain sections stained with H&E or Crystal Violet (CV). **D)** *Nuak1*^{+/-} mice lived as long as their WT littermates. **E)** Tau mRNA levels measured by qRT-PCR did not change in *Nuak1*^{+/-} mice in comparison with WT littermates (n=5). Data are represented as mean \pm s.d.m. ** $p < 0.01$. Student's T-test.

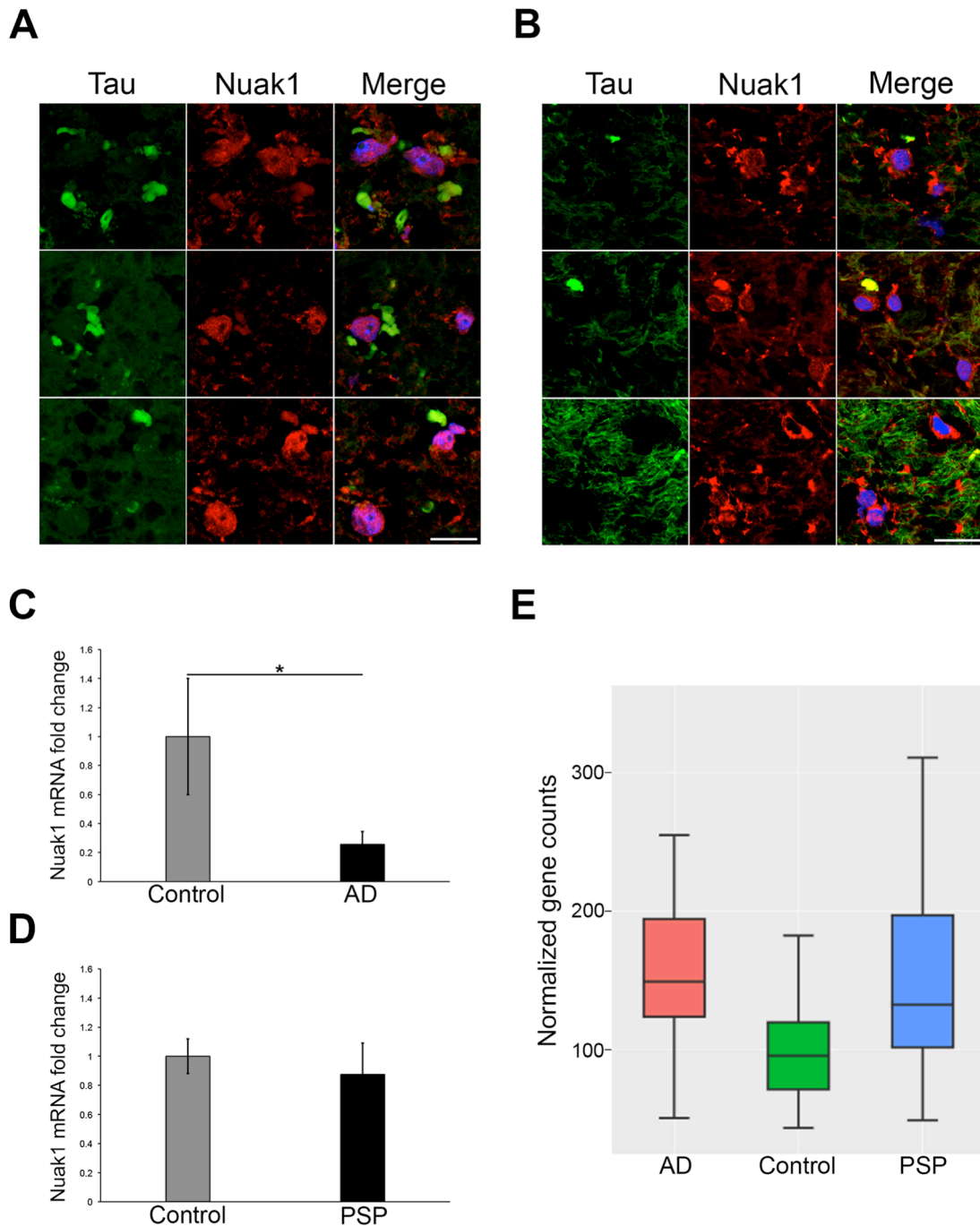


Figure S3, related to figure 2: Nuak1 in human tauopathies. A-B) Double staining of tau (green) and Nuak1 (red) in MFG (A) and pons (B) in healthy age-matched controls brain sections showed Nuak1 localization in the cytoplasm and nucleus. Scale bar, 15 μ m. **C)** Nuak1 mRNA levels measured by qRT-PCR decreased in AD cases in comparison with age-matched controls. **D)** Nuak1 mRNA levels measured by qRT-PCR did not change in PSP cases in comparison with age-matched controls. For all experiments, n=7, mean \pm s.d.m. *p<0.05. Student's T-test. **E)** RNA-seq data revealed no changes in Nuak1 mRNA levels between AD, PSP and age-matched control cases.

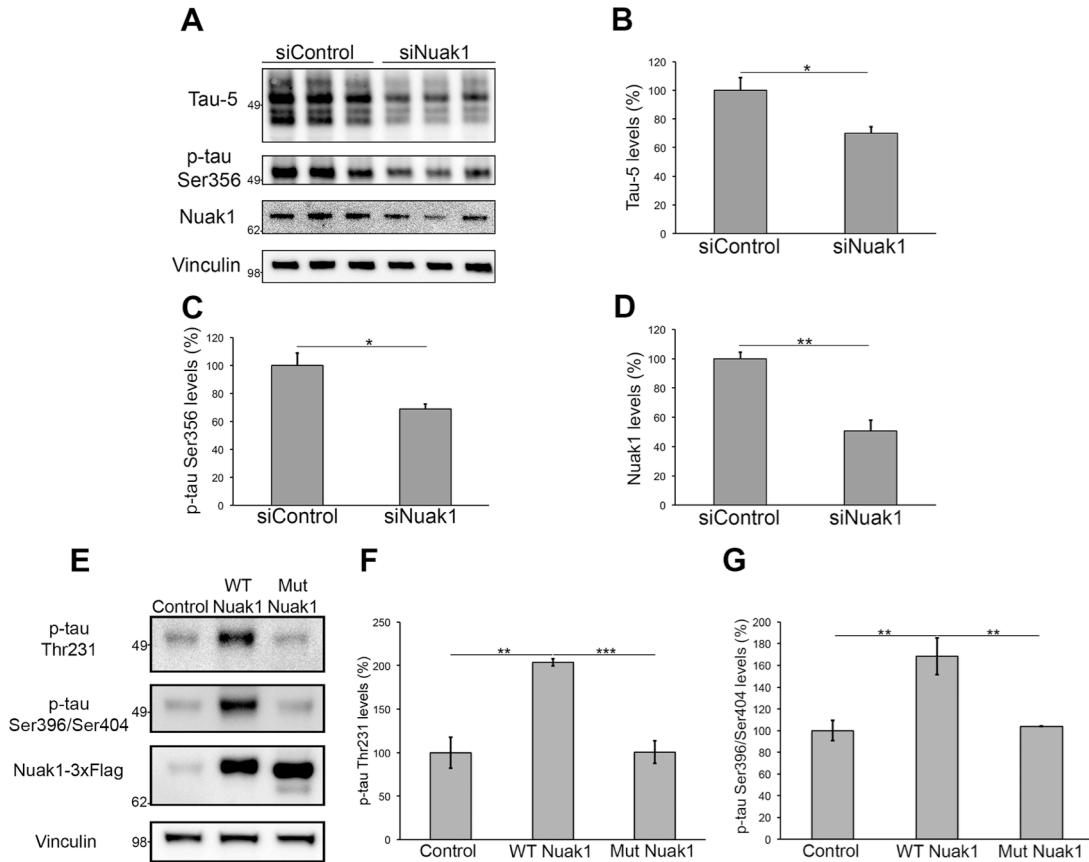


Figure S4, related to figure 3: Effects of Nuak1 over total and phospho-tau levels in neuroblastoma cells. **A)** Western blot analysis of extracts from neuroblastoma cells treated with siRNA for Nuak1 or control siRNA (n=6). **B)** Graph showing western blot quantification of total tau levels measured with tau-5 antibody. **C)** Graph showing western blot quantification of p-tau Ser356 levels. **D)** Graph showing western blot quantification of total Nuak1 levels. Data are represented as mean \pm s.d.m. **p<0.01, *p<0.05. Student's T-test. **E)** Western blot analysis of lysates from neuroblastoma cells transfected with active Nuak1-3xflag (WT Nuak1) or mutant K84M kinase dead Nuak1-3xflag (Mut Nuak1) (n=9). **F)** Graph showing western blot quantification of p-tau Thr231 levels. **G)** Graph showing western blot quantification of p-tau Ser396/Ser404 levels. For all quantifications, **p <0.01, ***p<0.001, ANOVA followed by Bonferroni's post hoc test.

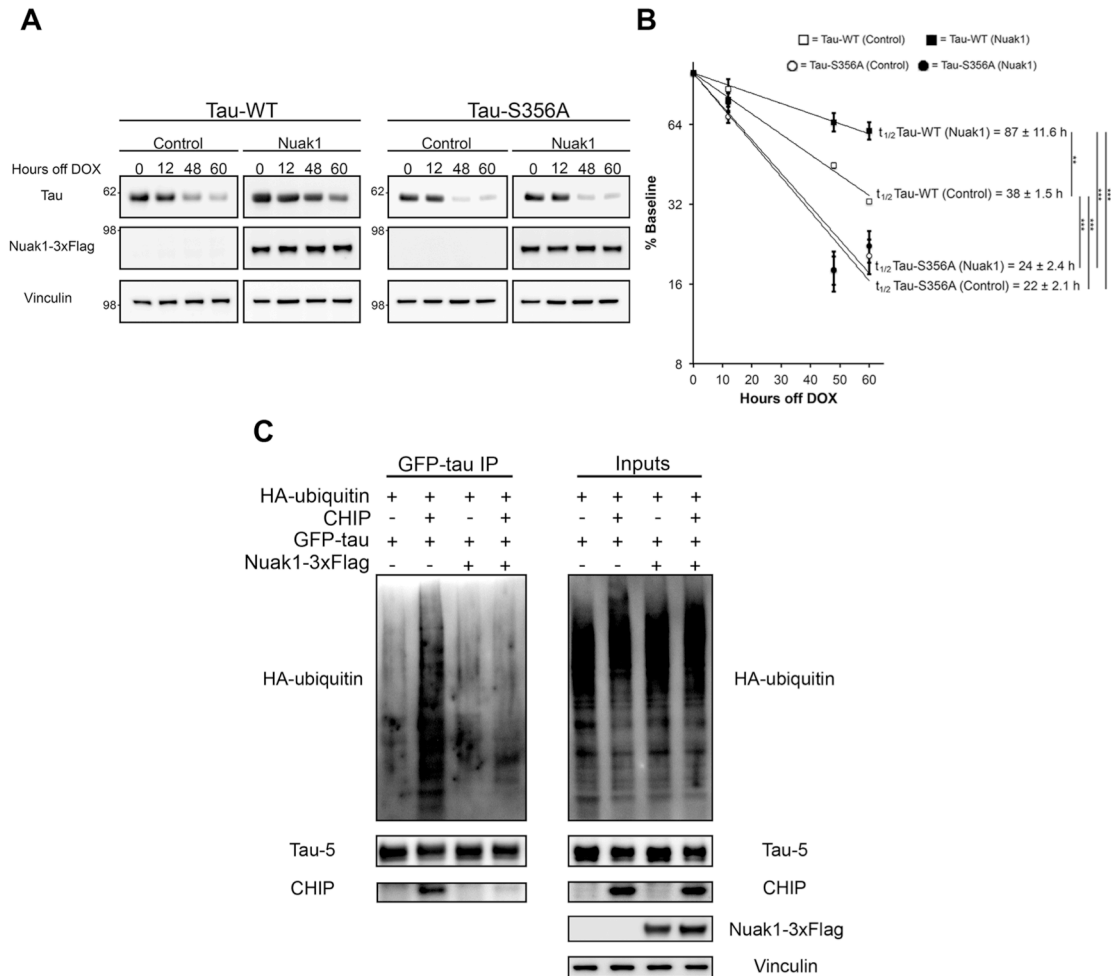


Figure S5, related to figure 3: Nuak1 stabilizes tau protein levels by phosphorylating tau at Ser356, decreasing tau ubiquitination and its binding to CHIP. **A)** Western blot analysis of lysates from doxycycline-inducible cell lines expressing either wild type tau or mutant S356A tau following different timepoints of doxycycline (DOX) removal, with or without Nuak1 over-expression. **B)** Graph showing western blot quantification of WT or mutant S356A tau stability. Graph is presented as a % of baseline and fit to a logarithmic (\log_2) scale ($n=5$). All half-life ($t_{1/2}$) quantifications are represented as mean \pm s.e.m. $**p < 0.01$, $***p < 0.001$, ANOVA followed by Bonferroni's post hoc test. **C)** Neuroblastoma cells were transfected with GFP-tau and cotransfected with CHIP, Nuak1-3xFlag, or both. GFP coimmunoprecipitation confirmed that CHIP bound to and greatly enhanced the ubiquitination of tau; however, Nuak1 prevented this interaction.

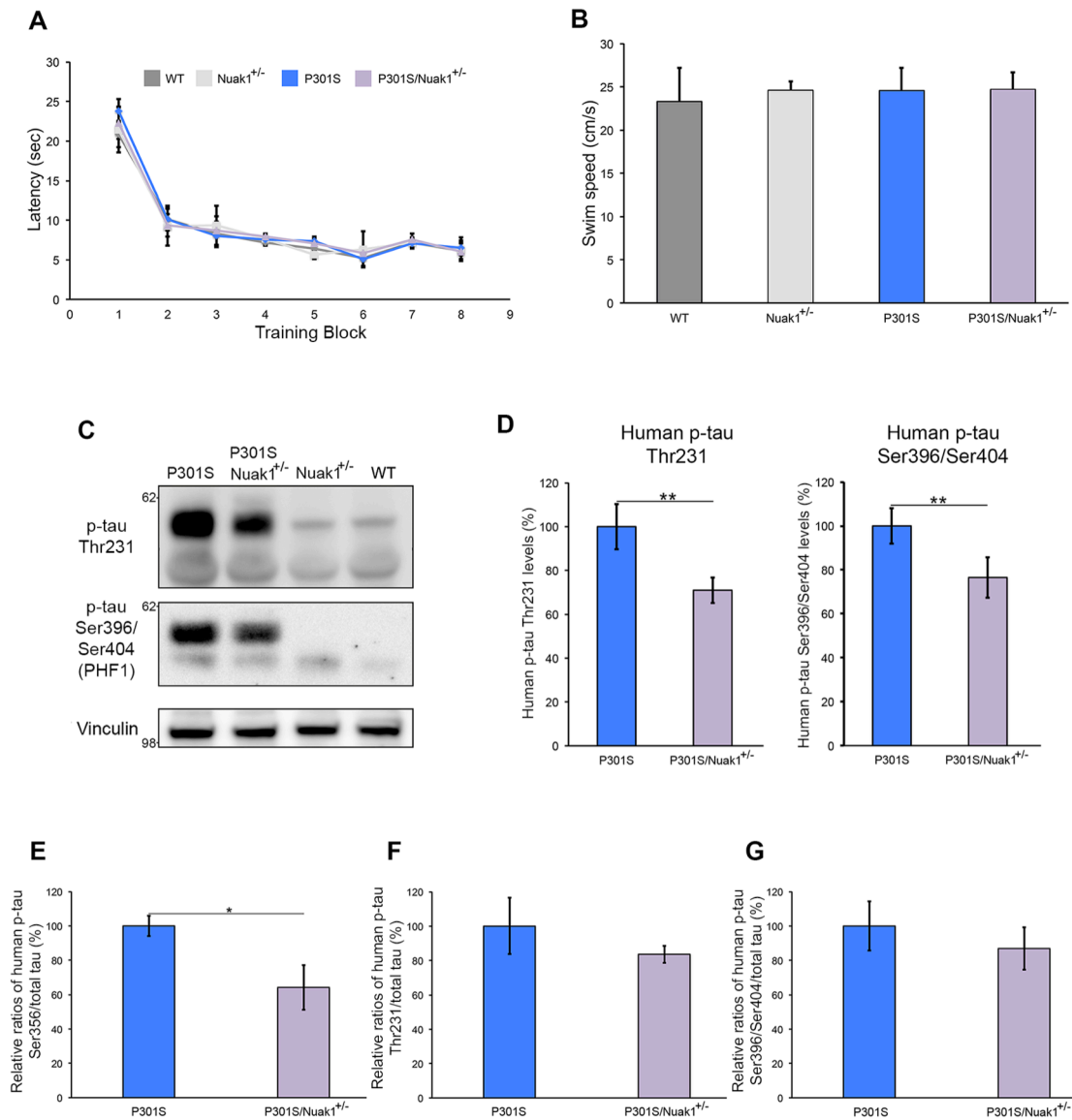


Figure S6, related to figures 4 and 5: Effects of Nuak1 downregulation in a tauopathy mouse model.

A) No difference between groups was observed during the visible platform training session. **B)** No differences in swim speed were observed between groups. **C)** Western blot analysis of brain homogenates from four different genotypes. **D)** Graphs showing western blot quantification of human p-tau Thr231 and p-tau Ser396/Ser404 levels. For all experiments, $n=8$, mean \pm s.d.m. $**p<0.01$. For western blot quantification we utilized ANOVA followed by Bonferroni's post hoc test. **E)** Graph showing relative ratios of p-tau Ser356 to total tau. **F)** Graph showing relative ratios of p-tau Thr231 to total tau. **G)** Graph showing relative ratios of p-tau Ser396/Ser404 to total tau. For all experiments, $n=8$, mean \pm s.d.m. $*p<0.05$.

Human brain samples

BRC #	FDX	CERAD	BRAAK	AGE	SEX	RACE	PMD	FR
2332	AD	C	6	88	F	W	17	MFG
2338	AD	C	6	87	M	W	7	MFG
2344	AD	C	5	86	M	W	5	MFG
2417	AD	B	6	61	F	W	5	MFG
2423	AD	B	6	89	F	W	7	MFG
2447	AD	C	6	65	M	W	11	MFG
2454	AD	C	6	62	F	W	18	MFG
2464	AD	C	6	52	M	W	4.5	MFG
2494	AD	C	4	81	F	W	15	MFG
2495	AD	C	5	67	M	W	6	MFG

BRC #	FDX	CERAD	BRAAK	AGE	SEX	RACE	PMD	FR
1553	PSP			77	F	W	8	PONS
1715	PSP			77	F	W	2	PONS
1798	PSP			76	F	W		PONS
1827	PSP			72	F	W	15	PONS
1831	PSP			72	M	W	11	PONS
2114	PSP	0	3	79	M	B	12	PONS
2121	PSP	0	4	85	M	W	7	PONS
2147	PSP	0	4	87	F	W	17	PONS
2159	PSP, CEREBROVASCULAR NOT CONTRIBUTING	0	0	74	F	W	20	PONS
2421	PSP, CEREBROVASCULAR DISEASE (NC)	0	4	66	M	W	9.5	PONS

BRC#	FDX	AGE	SEX	RACE	PMD	FRZ
0004	Control with few NFT	63	F	W	22	MFG PONS
0039	CONTROL	63	M	W	30-34	MFG PONS
0085	CONTROL, FEW NFT	65	F	B	33	MFG PONS
0107	CONTROL, OLD INFARCT	71	M	W	14	MFG PONS
0123	CONTROL, NFT ERC	80	F	W		MFG PONS
0155	CONTROL, min tau, old infarct	72	M	W	24	MFG PONS
0189	Control, NFT ERC	71	F	W	17	MFG PONS
0305	CONTROL	60	M	B	12	MFG PONS
0323	CONTROL	63	F	W	23	MFG PONS
0507	CONTROL	87	F	W	35	MFG PONS

Table S1, related to figure 2: Pathological and clinical information for post-mortem human brain samples. BRC#= Brain Research Center identification number, AD= Alzheimer disease case, PSP= Progressive Supranuclear Palsy cases PMD= Post mortem delay (hours) MFG= Middle frontal gyrus W= White, B= Black, M=Male, F= Female.

Video S1, related to figure 1: Climbing assay. Decreased levels of *Drosophila* Nuak1 homolog suppressed motor impairment in tau flies.

Supplemental Experimental Procedures

Drosophila climbing assay

Motor performance test was assessed as previously described (Park et al., 2013). hTau was expressed in the nervous system using elav-Gal4, crosses were performed at 28.5°C. Briefly, % of motor performance was calculated as the percentage of flies able to climb up 9 cm in 15 seconds (10 trials average).

Preparation of *Drosophila* protein lysates and immunoblot

Tau levels were analyzed in animals expressing tau in the adult eye under the control of Rh1-Gal4 that were aged 10 days at 28.5°C. Heads were collected and homogenized in LDS buffer (Life Technologies), 10% β-mercaptoethanol and loaded in 4-12% Bis-Tris gels, transferred to nitrocellulose membranes, blocked for one hour with 5% milk and incubated overnight with mouse monoclonal anti-Tau (clone T14, Life Technologies, RRID:AB_2533000) and anti-LaminC (Hybridoma bank LC2628).

Drosophila genotypes

Fig. 1C and Fig. S2A:

Control: w; GMR-Gal4/+

Tau/no modifier: w; GMR-Gal4, UAS-Tau19y/+

Tau/shNuak1: w; GMR-Gal4/+, UAS-Tau19y; P{GD7410}v16334/+

Fig. 1D:

Tau/no modifier: w; Rh1-Gal4/+; UAS-Tau31o/+

Tau/shNuak1: w; Rh1-Gal4/+; UAS-Tau31o/P{GD7410}v16334

Fig. 1E:

Control: Elav-Gal4/w; +; +

Tau: Elav-Gal4/+; +; UAS-Tau31o/+

Tau/shNuak1: Elav-Gal4/+; +; UAS-Tau31o/P{GD7410}v16334

Fig. S2B:

Control: Elav-Gal4/w; +; +

Control Nuak1^{OE}: Elav-Gal4/w; +; P{EPgy}CG43143^{EY22355}/+

Tau: Elav-Gal4/+; +; UAS-Tau31o/+

Tau/Nuak1^{OE}: Elav-Gal4/w; +; UAS-Tau31o/P{EPgy}CG43143^{EY22355}

Kinase assay

The *in vitro* kinase assay was performed using an ADP-Glo Kinase assay according to manufacturer's instructions (Promega, Cat # V9101). Briefly, this luminescent assay measured kinase activity by quantifying the amount of ADP produced during a kinase reaction. For the assay we utilized human recombinant tau 441 full-length protein, active wild-type human Nuak1 full-length protein, human Nuak1 without the kinase domain and human Caspase 6. The reaction was measured using an ELISA plate reader Synergy 2 from Biotek.

Mass Spectrometry analysis

The Mass Spectrometry-Proteomics Core Laboratory (MS-PCL) at Baylor College of Medicine analyzed samples from the kinase assay by LC-MS/MS using an AB SCIEX TripleTOF 5600 mass spectrometer.

RNA Extraction and Quantitative real-time PCR

Total RNA was obtained using the miRNeasy kit (Qiagen) according to the manufacturer's instructions. RNA was quantified using the NanoDrop 1000 (Thermo Fisher) and quality assessed by gel electrophoresis. cDNA was synthesized using Quantitect Reverse Transcription kit (Qiagen) starting from 1 µg of RNA. Quantitative RT-polymerase chain reaction (qRT-PCR) experiments were performed using the CFX96 Touch Real-Time PCR Detection System (Bio-Rad Laboratories) with PerfeCta SYBR Green FastMix, ROX (Quanta Biosciences). Real-time PCR results were analyzed using the comparative Ct method and normalized against housekeeping genes. The range of expression levels was determined by calculating the standard deviation of the Δ Ct (Pfaffl, 2001). Statistical significance was calculated using two-tailed Student t-test. Primers used to amplify specific exons of the human target genes were designed across introns to distinguished spliced cDNA from genomic contamination. Primer sequences are the following:

mmNuak1-Frwd: TCCAACCTGTACCAGAAGGAC

mmNuak1-Rev: GGCATCGTTCATAAATGAGA

mmNuak1-Frwd-II: CAGCCGAGTGGTTGCTATAA

mmNuak1-Rev-II: TGGTTGAGGGATGACATGATCT

mmTau-Frwd: TTCTCCTCCGCTGCCTCTT

mmTau-Rev: AGGGTCAGCCATACTGGTTC

mmTau-Frwd-II: CTTCTGTCTCGCCTTCTGT

mmTau-Rev-II: CTTCCATTGTGTCAAACCTCTG

mmS16-Frwd: AGGAGCGATTTGCTGGTGTGG

mmS16-Rev: GCTACCAGGGCCTTTGAGATG

hActB-Frwd: CCAGATCATGTTTGAGACCT

hActB-Rev: AGAGCGTACAGGGATAGCA

RNA-seq data

The results published here are in whole, or in part, based on data obtained from the Accelerating Medicines Partnership for Alzheimer's Disease (AMP-AD) Target Discovery Consortium data portal and can be accessed at doi:10.7303/syn2580853. Study data were provided by the following sources: The Mayo Clinic Alzheimers Disease Genetic Studies, led by Dr. Nilufer Taner and Dr. Steven G. Younkin, Mayo Clinic, Jacksonville, FL using samples from the Mayo Clinic Study of Aging, the Mayo Clinic Alzheimers Disease Research Center, and the Mayo Clinic Brain Bank. Data collection was supported through funding by NIA grants P50 AG016574, R01 AG032990, U01 AG046139, R01 AG018023, U01 AG006576, U01 AG006786, R01 AG025711, R01 AG017216, R01 AG003949, NINDS grant R01 NS080820, CurePSP Foundation, and support from Mayo Foundation. Study data includes samples collected through the Sun Health Research Institute Brain and Body Donation Program of Sun City, Arizona. The Brain and Body Donation Program is supported by the National Institute of Neurological Disorders and Stroke (U24 NS072026 National Brain and Tissue Resource for Parkinsons Disease and Related Disorders), the National Institute on Aging (P30 AG19610 Arizona Alzheimers Disease Core Center), the Arizona Department of Health Services (contract 211002, Arizona Alzheimers Research Center), the Arizona Biomedical Research Commission (contracts 4001, 0011, 05-901 and 1001 to the Arizona Parkinson's Disease Consortium) and the Michael J. Fox Foundation for Parkinsons Research.

RNA-seq experiments were performed using cerebellum. Number of cases: AD=82, PSP=84 and age match controls=79.

Stability assay

SH-SY5Y cell lines (RRID:CVCL_0019) stably expressing WT tau or mutant S356A tau were generated using the pINDUCER system (Meerbrey et al., 2011). Stable cell lines were selected for more than a week in geneticin-containing medium (G418, 150 µg/mL). Cells in 24 well plates were transfected with Nuak1-3xFlag (or empty plasmid) as described in the experimental procedures section and treated with doxycycline (DOX, 100 ng/mL) for 36 hours. DOX-containing media was replaced with DOX-free media at different time points. Cells were lysated as described in the experimental procedures section for western-blot assay. Image J was utilized to calculate protein half-lives as previously described (Li et al., 2004).

Coimmunoprecipitation and ubiquitination assay

In 24-well plates, neuroblastoma cell lines were transfected using Lipofectamine 200 with a combination of HA-ubiquitin (gift of E. Yeh, Addgene plasmid no 18712), GFP-tau, CHIP (GE-Dharmacon, clone ID 3847168) and Nuak1-3xFlag and maintained in complete media for 48 hours. Coimmunoprecipitation to assess GFP-tau ubiquitination and its binding to CHIP was performed using GFP-antibodies coated with dynabeads according to manufacturer's instructions (Chromotek, Cat # gtm-10). Samples were subjected to western blot analysis and probed using antibodies for tau (tau-5, 1:1000, abcam), CHIP (1:1000, abcam, RRID:AB_303412) and HA (1:1000, abcam, RRID:AB_444303).

Mouse brain Immunohistochemistry (IHC)

Immunohistochemistry was performed on paraffin-embedded sections. In brief, sections (5 µm) were deparaffinized and rehydrated. After blocking in normal goat serum for 1 hr, sections were incubated overnight with PHF1 antibody (1:100). The next day, the sections were washed in PBS 1X 3 times for 10 min each time and then incubated with biotinylated goat anti-mouse IgG and visualized using an ABC reagent kit (Vector Laboratories, RRID:AB_2336827) according to the manufacturer's recommendations. Bright-field images were acquired using a Carl Zeiss Axio Imager M2 microscope, equipped with an Axio Cam MRc5 color camera (Carl Zeiss, Germany). Sections were counterstained with hematoxylin (Vector Laboratories, RRID:AB2336842) for nuclear staining.

REFERENCES

- Li, W., Lesuisse, C., Xu, Y., Troncoso, J.C., Price, D.L., and Lee, M.K. (2004). Stabilization of alpha-synuclein protein with aging and familial parkinson's disease-linked A53T mutation. *The Journal of neuroscience : the official journal of the Society for Neuroscience* 24, 7400-7409.
- Meerbrey, K.L., Hu, G., Kessler, J.D., Roarty, K., Li, M.Z., Fang, J.E., Herschkowitz, J.I., Burrows, A.E., Ciccia, A., Sun, T., *et al.* (2011). The pINDUCER lentiviral toolkit for inducible RNA interference in vitro and in vivo. *Proceedings of the National Academy of Sciences of the United States of America* 108, 3665-3670.
- Pfaffl, M.W. (2001). A new mathematical model for relative quantification in real-time RT-PCR. *Nucleic acids research* 29, e45.